Geosciences Journal
Vol. 7, No. 3, p. 277 − 288, September 2003

Chemical weathering and climate – a global experiment: A review

Youngsook Huh* *Department of Geological Sciences, Northwestern University, Evanston, IL 60208-2150, U.S.A.*

ABSTRACT: How has the Earth maintained a habitable environment while its closest neighbors, Venus and Mars, are currently too hot or too cold? This fortunate state has been attributed to a negative feedback hypothesis that has stood unchallenged for years. In this model, any increase in atmospheric CO_2 production is balanced by increased CO_2 uptake by silicate weathering under greenhouse conditions. A decrease in atmospheric CO_2, then, is balanced by decreased silicate weathering rates under the colder climate. A global experiment utilizing published geochemical data from large rivers at different latitudes helps us test the climate dependence of weathering, central to this hypothesis. When rivers draining granitic shields and basaltic provinces are compared, there is no systematic latitudinal variation (temperature dependence) in the rates of chemical weathering. At global scale the physical mechanisms superimpose a threshold effect on the underlying climate-dependence of silicate weathering. On tropical cratons, the buildup of lateritic regolith suppresses weathering. In the arctic/subarctic, frost action efficiently removes the regolith and generates physical exposure of silicate rocks to the weathering agents (water, CO_2), thereby accelerating reaction. Available field observations do not support the currently standard Clausius-Clapeyron-Arrhenius model.

Key words: rivers, carbon dioxide, carbon cycle, silicate, Arrhenius

1. INTRODUCTION

Geochemical models of the evolution of Phanerozoic atmospheric CO_2 assume that the silicate weathering rate is a positive, smoothly increasing function of CO_2 (Walker et al., 1981). The two are coupled through increase in metabolic rates and more vigorous hydrologic cycle caused by the greenhouse effect of CO_2. Thermodynamically, the Clausius-Clapeyron relationship describes the rapid increase of the saturation vapor pressure of water (P_{H_2O}) with increasing temperature:

$$P_{H_2O} = Ce^{-(\Delta H_{vap}/RT)} \quad (1)$$

where ΔH_{vap} is the enthalpy of vaporization (kJ/mol), T is temperature (K), R is gas constant (kJ/mol/K), and C is a constant. Environmental measurements show ~6% increase in P_{H_2O} per °C at tropical temperatures (Webster, 1994). The result is an increase in precipitation and hence vegetative cover, metabolic soil CO_2, and the availability of protons for weathering.

*Corresponding author: huh@earth.northwestern.edu

$$CO_2 + H_2O \rightleftharpoons \underset{\text{carbonic acid}}{H_2CO_3} \rightleftharpoons H^+ + \underset{\text{bicarbonate}}{HCO_3^-} \quad (2)$$

Kinetically, the Arrhenius law states that reaction rates increase exponentially with increasing temperature:

$$Rate = Ae^{-(Ea/RT)} \quad (3)$$

where E_a is the apparent activation energy (kJ/mol), and A is a constant. Laboratory dissolution experiments are in accord, with E_a of ~50 kJ/mol for albite and K-feldspar (White and Brantley, 1995). Thus, variations in temperature over multimillion year timescales induced by changing levels of atmospheric CO_2 lead to shifts in (1) water vapor pressure, precipitation, runoff and (2) metabolic and chemical weathering kinetics. In this manner, the drawdown of CO_2 by silicate weathering provides a negative feedback to the initial change in P_{CO_2}.

Models of the geochemical carbon cycle incorporate this negative feedback through an Arrhenius function with E_a for Ca- and Mg-silicate weathering determined from laboratory experiments (63 kJ/mol; Berner and Kothavala, 2001). According to this, assuming average summer temperatures of 10°C for the arctic/subarctic and 28°C for the tropics, the weathering rates should be about 5 times higher at lower latitudes. A difference of this magnitude would be readily observed in the field data. To field-test the hypothesis on the global scale relevant for geochemical carbon cycle models, I present a comparative study of the large rivers of the world at different latitudes.

2. THE STRATEGY

2.1. Weathering Reactions

In the inorganic carbon cycle, the primary input terms for atmospheric CO_2 are mantle outgassing from mid-ocean ridges, hot spots, and andesite volcanoes on active margins and the recycled component by metamorphic breakdown of carbonates (Reaction 4) in active orogenies in oceanic and continental arcs and collision zones (Fig. 1).

$$CaCO_3 + SiO_2 \rightleftharpoons CaSiO_3 + CO_2 \quad (4)$$

Reaction 4 is a schematic representation of the tendency for calcium carbonate to react with degraded aluminosilicates at intermediate temperatures (~150°C) in a water sat-

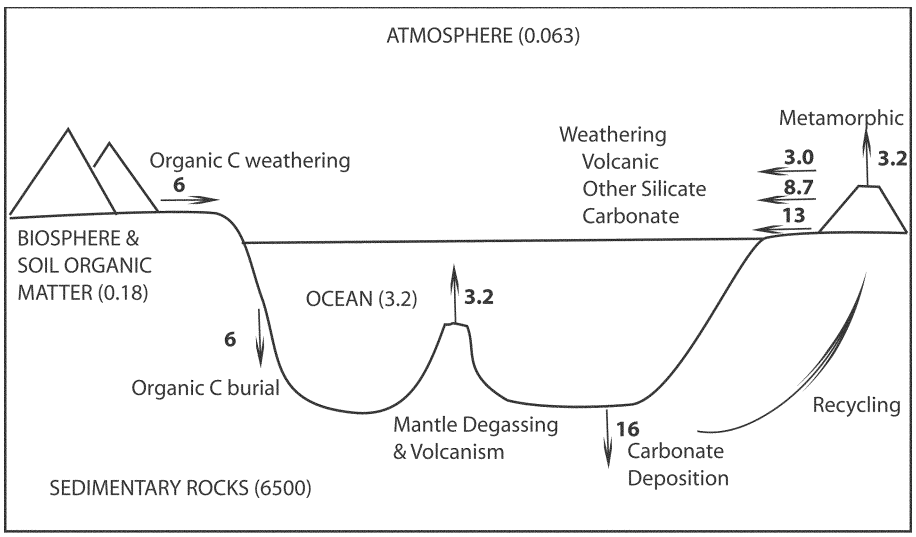

Fig. 1. The present-day state of the global long-term carbon cycle. Reservoir sizes (10^{18} mol C) are in parentheses (Mackenzie, 2003). The major reservoirs are (i) the combined atmosphere-ocean-biosphere and (ii) the sedimentary rocks. Fluxes (10^{12} mol C/y) are in bold (Wallmann, 2001).

urated environment to produce Ca-silicates and CO_2. The two major CO_2 consuming weathering reactions are (1) the congruent (i.e., complete) dissolution of the major carbonates (Reactions 2 and 5) and (2) the incongruent degradation of the high temperature aluminosilicate minerals in igneous and metamorphic rocks to residual clays, dissolved cations, and silica (e.g., Reactions 2, 6 and 7).

$$\underset{\text{calcite}}{CaCO_3} + \mathbf{H^+} \rightleftharpoons Ca^{2+} + HCO_3^- \quad (5)$$

$$7\underset{\text{albite}}{NaAlSi_3O_8} + \mathbf{6H^+} + 20H_2O \rightleftharpoons 6Na^+ + 10\underset{\text{silica}}{Si(OH)_4} + 3\underset{\text{montmorillonite}}{Na_{0.33}Al_{2.33}Si_{3.67}O_{10}(OH)_2} \quad (6)$$

$$6\underset{\text{montmorillonite}}{Na_{0.33}Al_{2.33}Si_{3.67}O_{10}(OH)_2} + \mathbf{2H^+} + 23H_2O \rightleftharpoons 2Na^+ + 8Si(OH)_4 + 7\underset{\text{kaolinite}}{Al_2Si_2O_5(OH)_4} \quad (7)$$

Reactions 6 and 7 can be regarded crudely as simple ion exchange of the protons produced from hydration of CO_2 (Reaction 2) with the cations contained in the lattice positions of the minerals (in this case, Na^+). Ion exchange of protons results in structural rearrangements, accompanied by the loss of some silica to solution, to form clays with Na/Al and Si/Al ratios lower than the original minerals. These clays are much closer to thermodynamic equilibrium at Earth surface conditions than were the original high temperature igneous and metamorphic phases.

For the climate not to descend into a permanent "ice-house" state, it would appear that the weathering reactions must be easily and rapidly reversible, as is the case for calcite. Reaction 5 is reversed by the biogenic formation of calcareous tests and other structures and by simple inorganic precipitation. The biological precipitation is limited by the availability of the minor, essential nutrients, nitrate, phosphate and, perhaps, iron. The upper oceans are generally saturated with the two dominant phases of $CaCO_3$, calcite and aragonite. As simple salts, these phases will precipitate spontaneously at greater than ~400% super-saturation in the absence of biological activity (Berner, 1978). Only in very dilute, low alkalinity lakes is there evidence for a carbon limitation in aquatic systems. Thus, as Reaction 5 is reversible in the time frame of interest here (multimillion years) there is no net consumption of CO_2 by weathering of carbonates. At the other extreme, for the Earth not to evolve into a Venus-like CO_2 "hothouse", there must be mechanisms that balance the observed mantle and metamorphic outgassing of CO_2 and prevent it from accumulating to very high levels. Silicate weathering process is the only long-term sink and is crucial in determining the surface environmental conditions of the Earth.

2.2. Data Source

Here the focus is on rivers draining granitic and basaltic terrain, but similar comparisons for sedimentary and orogenic zones can be found in Edmond and Huh (1997) and Huh et al. (1998a,b). Extensive data sets from pristine tropical systems with granitic bedrock are available for the Amazon draining the Brazilian Shield (Stallard and Edmond, 1983), Orinoco draining the Guayana Shield (Edmond et al., 1995), and the rivers in Cameroon and Congo draining the Congo Shield (Négrel et al., 1993; Viers et al., 2000) (Fig. 2). Unfortunately, rivers in temperate zones have been impacted by human activity, and most of the Northern Hemisphere landscapes are dominated by recent glacial action. Data for high latitudes are from the Mackenzie and St. Lawrence draining the Canadian Shield (Millot et al., 2002). These Canadian basins have glacial overburden, some from outside the drainage basins, which may obscure the primary signal from contemporary in-situ weathering of

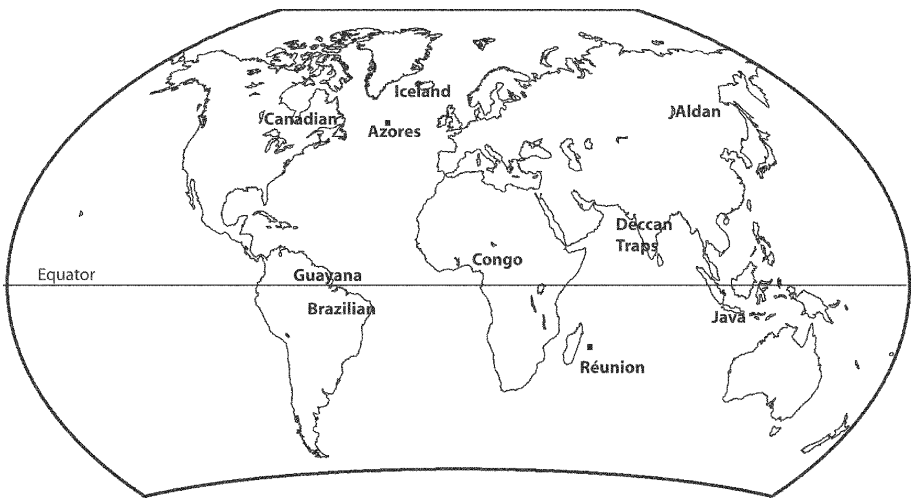

Fig. 2. Location of shields and basaltic provinces discussed in the text.

basement rocks. In this respect, the rivers of Eastern Siberia draining the Aldan Shield (Huh and Edmond, 1999) are useful. Eastern Siberia was free from extensive glaciation during the ice advances owing to the semi-arid climate and precipitation occurring generally as rain in summer. Data for basaltic terrains are from the Réunion island (Louvat and Allègre, 1997), Sao Miguel volcanic island in the Azores (Louvat and Allègre, 1998), Iceland (Louvat, 1997), Java (Louvat, 1997), and from the flood basalts of Deccan Traps in India (Dessert et al., 2001).

2.3. Major Elements and Strontium Isotopic Composition

Rivers integrate weathering product of all lithologies in the drainage basin. Therefore the proportion of dissolved load generated by CO_2-consuming silicate weathering reactions (Reactions 6 and 7) should be distinguished from non-CO_2 consuming ones by carbonates (Reaction 5) and evaporites (Reactions 8 and 9).

$$\underset{\text{halite}}{NaCl} \rightleftharpoons Na^+ + Cl^- \tag{8}$$

$$\underset{\text{gypsum}}{CaSO_4 \cdot 2H_2O} \rightleftharpoons Ca^{2+} + SO_4^{2-} + 2H_2O \tag{9}$$

Ternary diagrams as in Figure 3 enable one to visualize the relative contribution of different lithologies. Carbonate weathering will manifest itself on such diagrams as points clustered near the Ca and HCO_3 apices (Reaction 5) and evaporites around ($Cl+SO_4$) apex (Reactions 8 and 9). Data falling in the interior of the anion ternary diagram indicate contributions from oxidative weathering of pyritic shales (Reactions 10 and 5, 6 and 7).

$$\underset{\text{pyrite}}{2FeS_2} + 7.5O_2 + 4H_2O \rightleftharpoons Fe_2O_3 + 4SO_4^{2-} + \mathbf{8H^+} \tag{10}$$

The tropical shield data fall on a trend from close to the (Na+K) apex to the central part of the cation ternary diagram (Fig. 3a). That estimates of the composition for average igneous rock types (Wedepohl, 1995) show a similar trend (Fig. 3b) suggests that weathering reactions go to completion with little retention of major cations in residual clays. The presence of significant amounts of organic acids in these rivers makes alkalinities very low or even negative. Therefore anion ternary diagrams are not plotted. Arctic/subarctic shields have higher abundances of Ca and Mg than Na and K; alkalinity is the dominant anion with minor Si (Fig. 3c). This indicates that weathering is superficial, i.e. exchange of surficial cations for protons with little clay formation. Canadian Shield data are of rivers draining western (Mackenzie system) and eastern (St. Lawrence system) parts of the shield. The latter are high in dissolved organic carbon (10 to 52 mg/l), and there is a large imbalance between total major cation and anion concentrations (30 to 60% imbalance) (Millot et al., 2002). The implication is that, like in the tropical shield rivers, organic anions make a significant contribution, and thus the data plot in a separate field on the anion ternary diagram. The basaltic rivers are more magnesian and high in Si (Fig. 3d). On the anion diagram, a range from cation-poor siliceous rocks to carbonate to shale/evaporite contributions are demonstrated.

Strontium isotopes add another level of lithologic constraint. $^{87}Sr/^{86}Sr$ ratio of seawater for the past 500 Ma recorded in marine limestones has varied between 0.7065 and 0.7095, and weathering of marine carbonates and evaporites is expected to yield values in this range. The fast dissolution of carbonates and evaporites render the dissolved $^{87}Sr/^{86}Sr$ ratio sensitive to the amount of those minerals present in the drainage basin. Weathering of old aluminosilicate rocks generates radiogenic but highly variable isotope ratios depending on the content of the parent element, Rb, and age. The resulting dissolved Sr concentrations are low because of the slow weathering kinetics. On the Guayana Shield the whole rock $^{87}Sr/^{86}Sr$ ratios are 0.75 to 0.90 in potassic granites, and river dissolved $^{87}Sr/^{86}Sr$ values range up to 0.9 (Fig. 4). The

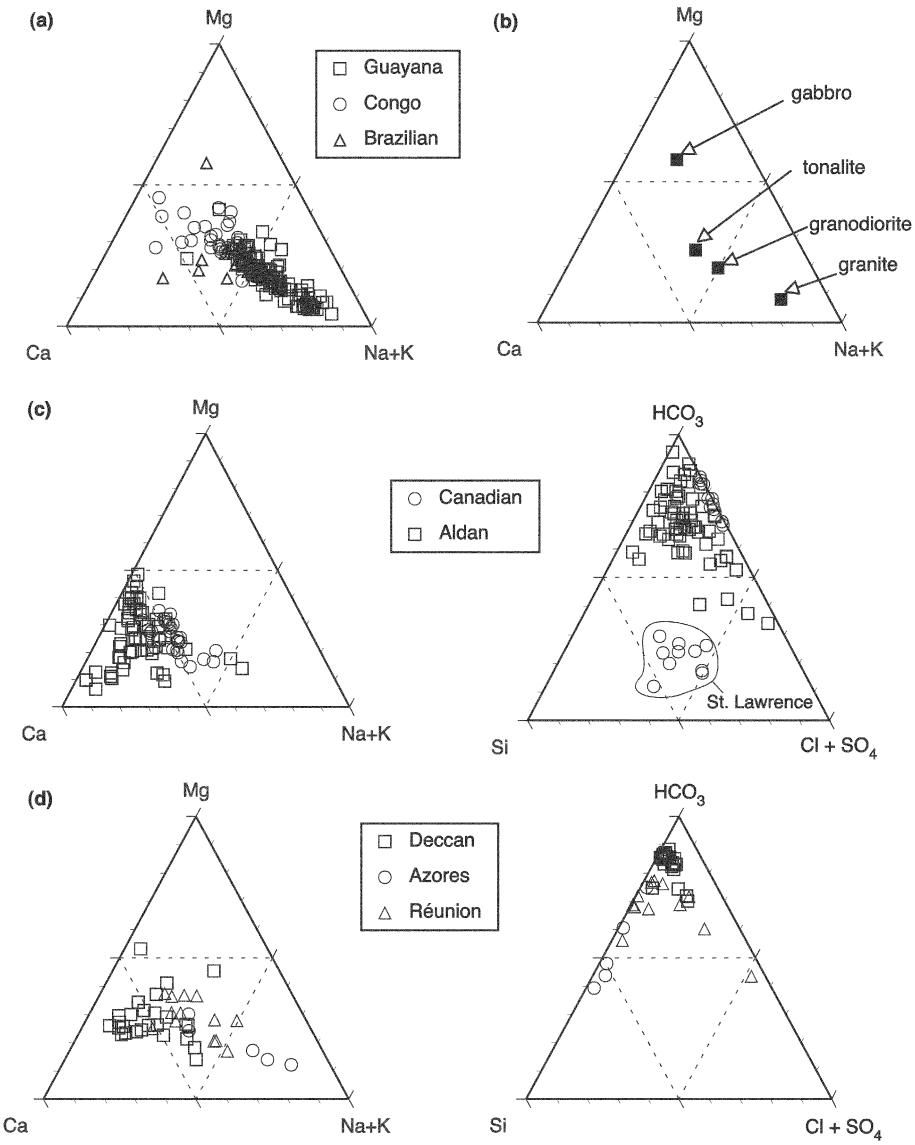

Fig. 3. A compilation of ternary plots for rivers draining continental shields. The ternary diagrams show element ratios rather than absolute concentrations that are dependent on water discharge. (**a**) Tropical shields: the Brazilian (Stallard and Edmond, 1983), Guayana (Edmond et al., 1995), and Congo (Viers et al., 2000). (**b**) Average igneous rock composition (Wedepohl, 1995). (**c**) High latitude shields: Canadian (Millot et al., 2002) and Aldan (Huh and Edmond, 1999). (**d**) Basaltic provinces: the Deccan Traps (Dessert et al., 2001), Sao Miguel (Louvat and Allègre, 1998), and Réunion (Louvat and Allègre, 1997). Data are corrected for marine aerosol input.

Rb/Sr systematics in the dissolved load follow a "fluvial isochron" concordant with whole rock (Edmond et al., 1995). In contrast, the rocks are strongly metamorphosed to granulite facies on much of the Aldan Shield. Thus, the Rb abundances are low and as a result the whole rock $^{87}Sr/^{86}Sr$ ratios are relatively non-radiogenic (up to 0.75 in granite gneiss assemblage) (Vinogradov and Leytes, 1987). The river dissolved $^{87}Sr/^{86}Sr$ range to 0.720. Rivers draining other high latitude shields, the Baltic (Åberg and Wickman, 1987; Wickman and Åberg, 1987; Andersson et al., 1994) and the Canadian (Wadleigh et al., 1985; Yang et al., 1996; Millot et al., 2002), are similarly not highly radiogenic. Young volcanic rocks yield unradiogenic values and relatively high concentrations.

Complications to the interpretation of river dissolved $^{87}Sr/^{86}Sr$ arise from disseminated calcite (White et al., 1999), hydrothermal or metamorphic carbonates that inherit radiogenic Sr from surrounding rocks (Palmer and Edmond, 1992), and preferential dissolution of radiogenic Sr in biotite (Blum and Erel, 1995). Their effect at regional scales is difficult to gauge and cannot be avoided even at smaller spatial scales. Thus, $^{87}Sr/^{86}Sr$ data should be interpreted with care in combination with ancillary chemical data and lithological information.

2.4. Rates of CO_2 Uptake by Silicate Weathering

The total dissolved flux (tons/y or mol/y) or yield (tons/km^2/y or mol/km^2/y) can be calculated using major element concentrations, mean annual discharge, and drainage basin area. One can estimate the consumption rate of CO_2 by silicate weathering (ϕCO_2, mol/y) by assuming a relationship between ϕCO_2 and flux of total dissolved cations ($\phi TZ^+ = \phi Na^+ + \phi K^+ + 2\phi Mg^{2+} + 2\phi Ca^{2+}$, charge equivalents/y), bicarbonate (ϕHCO_3, mol/y), or dissolved silica (ϕSi, mol/y) (Table 1). The justification comes from Reactions 2, 6 and 7, where $CO_2:H^+:Na^+ = 1:1:1$ or $CO_2:H^+:HCO_3^- = 1:1:1$ relationships hold. In

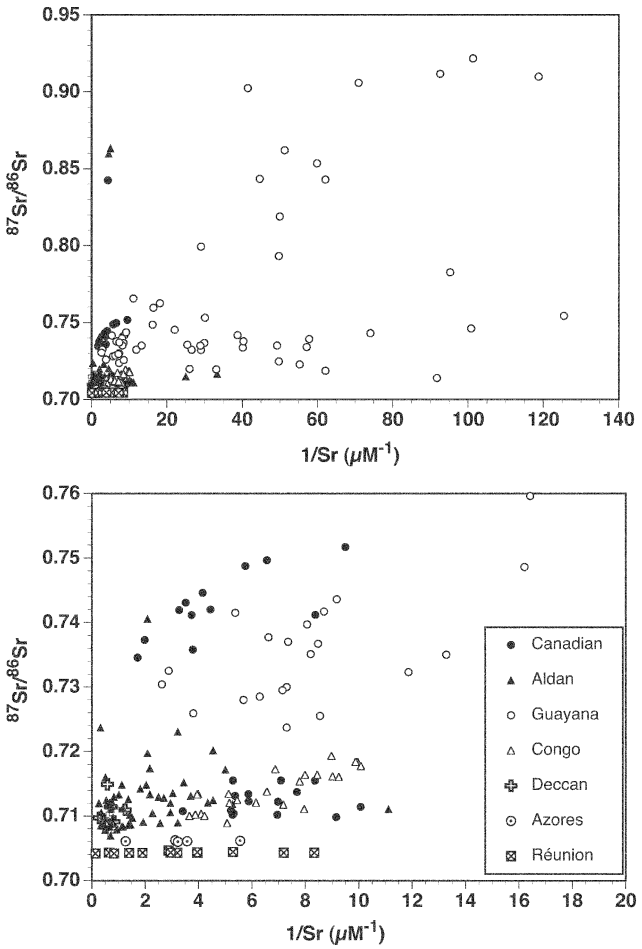

Fig. 4. Dissolved $^{87}Sr/^{86}Sr$ data for the shield rivers. Data sources are same as in Fig. 3. Present seawater value is 0.7091, and average riverine ratio is 0.712 (Palmer and Edmond, 1989). Weathering of marine carbonates/evaporites is expected to yield dissolved $^{87}Sr/^{86}Sr$ between 0.7065 and 0.7095 depending on age.

the case where small quantities of marine carbonates are present (as determined by close to marine $^{87}Sr/^{86}Sr$), recourse is made to ϕSi. $\phi CO_2 = 2\phi Si$ is borne out both from Reactions 6 and 7 and global fluvial Si data (Berner et al., 1983). Silica is involved in biological cycling and if there are lakes or reservoirs where uptake by diatoms occurs, use of the former relationship could underestimate ϕCO_2.

Allègre's group in France has championed the use of the inversion method to quantify the proportions of the total dissolved load contributed by weathering of each of the lithologies (carbonate, evaporite, silicate) (Négrel et al., 1993). The mixing equations for element X (Ca, Mg, HCO_3, and Cl) and $^{87}Sr/^{86}Sr$ are:

$$\left(\frac{X}{Na}\right)_{river} = \sum_i \left(\frac{X}{Na}\right)_i \alpha_{i,Na} \quad (11)$$

$$\left(\frac{^{87}Sr}{^{86}Sr}\right)_{river} \left(\frac{Sr}{Na}\right)_{river} = \sum_i \left(\frac{^{87}Sr}{^{86}Sr}\right)_i \left(\frac{Sr}{Na}\right)_i \alpha_{i,Na} \quad (12)$$

The $\alpha_{i,Na}$ are mixing proportions of Na from different reservoirs (i=rainwater, silicate, carbonate, evaporite). Starting with a set of *a priori* parameters, successive iterations produce a best fit to the whole set of equations. End-member compositions $(X/Na)_i$ and mixing proportions (α_i) are the output results.

The resulting weathering rate comparisons, processed by two different research groups, are shown in Figures 5 and 6. Both show a lack of any systematic change in weathering rate as a function of latitude or temperature. On the Aldan Shield, for example, freezing temperatures persist for ~200 days of the year. Monthly mean temperatures vary from ~15°C in July to ~ –50°C in February. The region is semi-arid with an average rainfall of ~550 mm/y. That such a basin should weather at similar rates as the Guayana Shield where the temperature is ~28°C and precipitation is ~3,000 mm/y is counter-intuitive at first. Based on the processes known, I examine the reason below.

3. DISCUSSION

3.1. Physical Factors: Lateritic Cover versus Frost Shattering

In the absence of a mechanism to create relief, i.e. exposure, aluminosilicate weathering is self-limiting, because it is incongruent. As the weathering front migrates vertically through the fresh rock, cations and silica dissolve and refractory aluminous phases accumulate (Twidale, 1990; Thomas, 1994) (Fig. 7). Conditions become anoxic (Reaction 13) and reducing (Reaction 14), allowing the mobilization of ferrous iron in solution (Bourman, 1993; Ambrosi and Nahon, 1986).

Table 1. Strategy for calculating CO_2 uptake by aluminosilicate weathering.

Geological terrains	ϕCO_2
Pure aluminosilicate-low organic acids	$\phi CO_2 = \phi TZ^+$ or $\phi CO_2 = \phi HCO_3$
Pure aluminosilicate-tropical "black" rivers	$\phi CO_2 = \phi TZ^+$
Mixed lithology-no lakes	$\phi CO_2 = 2\phi Si$
Mixed lithology-lakes, bogs, reservoirs	$\phi CO_2 = \phi TZ^+$ (if $^{87}Sr/^{86}Sr$>0.7100 or <0.7065)
	$\phi CO_2 = 2\phi Si$ (if 0.7065<$^{87}Sr/^{86}Sr$<0.7100)

$TZ^+ = Na^+ + K^+ + 2Ca^{2+} + 2Mg^{2+}$.
All parameters are corrected for atmospheric input of marine aerosols.

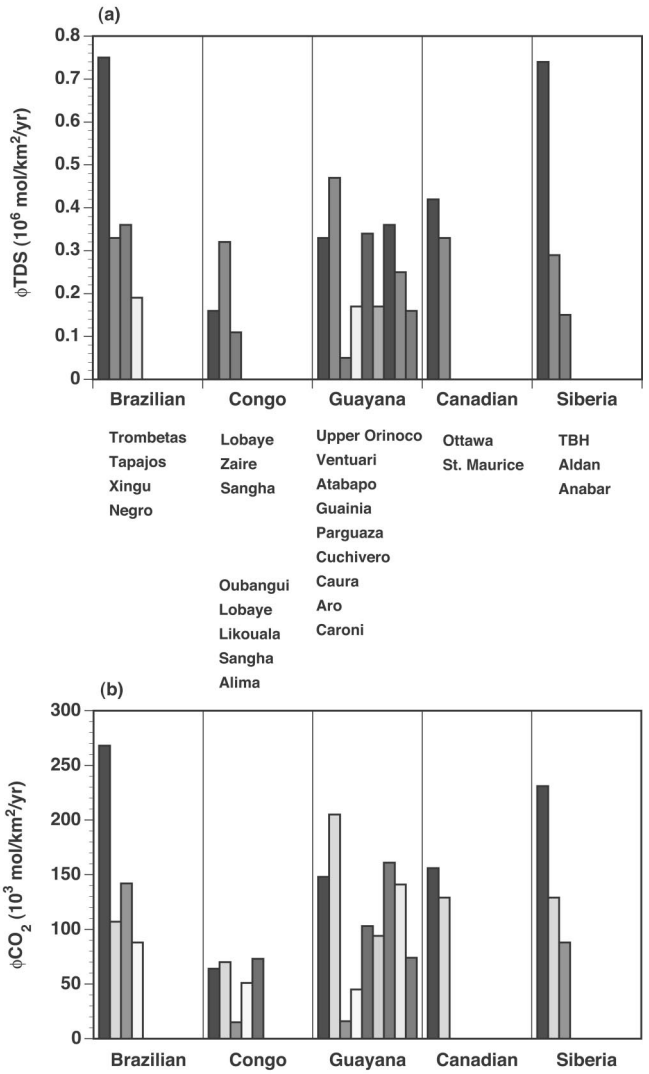

Fig. 5. (**a**) The flux of total dissolved solids (TDS = Na + K + Mg + Ca + Cl + SO_4 + HCO_3 + Si; mol/l) (**b**) CO_2 uptake rate as calculated according to the scheme in Table 1. Individual bars indicate different tributary systems within a watershed, names of which are listed under the bars. On the left are tropical rivers and on the right are the subarctic/arctic rivers. Figure from Huh and Edmond (1999).

$$\underset{\text{organics}}{C(H_2O)} + O_2 \rightleftarrows CO_2 + H_2O \tag{13}$$

$$Fe_2SiO_4 + 4CO_2 + 4H_2O \rightleftarrows \underset{\text{reduced Fe (soluble)}}{2Fe^{2+}} + Si(OH)_4 + 4HCO_3^- \tag{14}$$

Lateral and vertical migration of the soluble reduced iron, whose chemistry is similar to Ca, through the refractory regolith to oxic soil sections leads to its oxidation to the insoluble ferric form (Fe^{3+}) and precipitation as a ferruginous cement (Bourman, 1993; Thomas, 1994).

$$4Fe^{2+} + O_2 + 10H_2O \rightleftarrows 4Fe(OH)_3 + 8H^+ \tag{15}$$

The extremely low soluble Fe^{2+} concentrations that result from this oxidation reaction drive the vertical diffusion gradient for the reduced species between the deep anoxic and shallow oxic environments. In seasonally arid regimes dissolved silica produced by Reactions 6, 7 and 14 in the weathered mantle is also transported and reprecipitated by surface and capillary evaporation to form a siliceous cement, silcrete (Ollier, 1991).

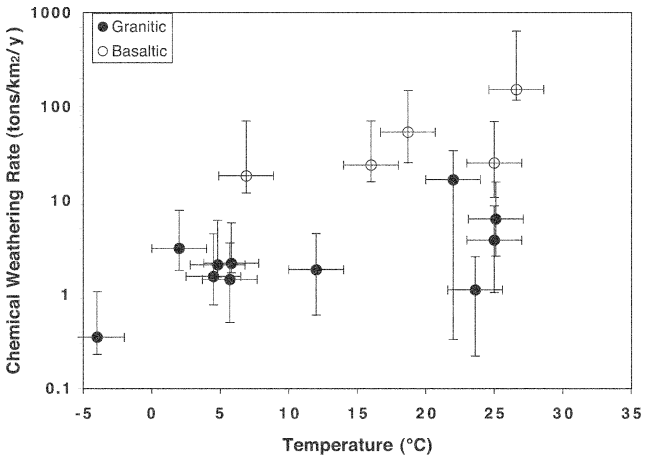

Fig. 6. Chemical weathering rates for rivers draining granitic and basaltic rocks plotted using values tabulated in Millot et al., 2002. Their data sources for granitic basins are Meybeck (1986), Martin (1987), McDowell and Asbury (1994), Vegas-Vilarrubia et al. (1994), Edmond et al. (1995), White and Blum (1995), Huh and Edmond (1999) and Viers et al. (2000). Data sources for basaltic basins are Louvat and Allègre (1997, 1998), Dessert et al. (2001) and Louvat (1997). The vertical bars indicate the range of values within the drainage basin. Chemical weathering rates are calculated as Chemical Weathering Rate = φNa + φK + φCa + φMg, where φ denotes flux. Because of the large uncertainties involved, Millot et al. (2002) did not consider it meaningful to calculate ϕCO_2.

$$\underset{\text{silcrete}}{Si(OH)_4} \rightleftarrows SiO_2 + 2H_2O \tag{16}$$

Thus, a regolith rich in silica and alumina (mostly as primary quartz and secondary kaolinite and gibbsite (Reactions 7 and 17), with a surface layer cemented with iron oxyhydroxides and silica (Reactions 15 and 16), accumulates and seals the fresh rock at the weathering front (Topp et al., 1984; Fig. 7).

$$\underset{\text{kaolinite}}{Al_2Si_2O_5(OH)_4} + 10H_2O \rightleftarrows \underset{\text{gibbsite}}{2Al(OH)_3} + 2Si(OH)_4 \tag{17}$$

Throughout this process, solifluction (semi-plastic flow) of the accumulating mantle further smoothes the surface relief leading to a progressive diminution in the hydraulic energy available for mechanical erosion and transport of the weathered overburden. The weathering yield on the Guayana Shield in the Orinoco River drainage is equivalent to an erosion rate of about 10 m/m.y. with equal mass fluxes of dissolved and suspended material (Edmond et al., 1995).

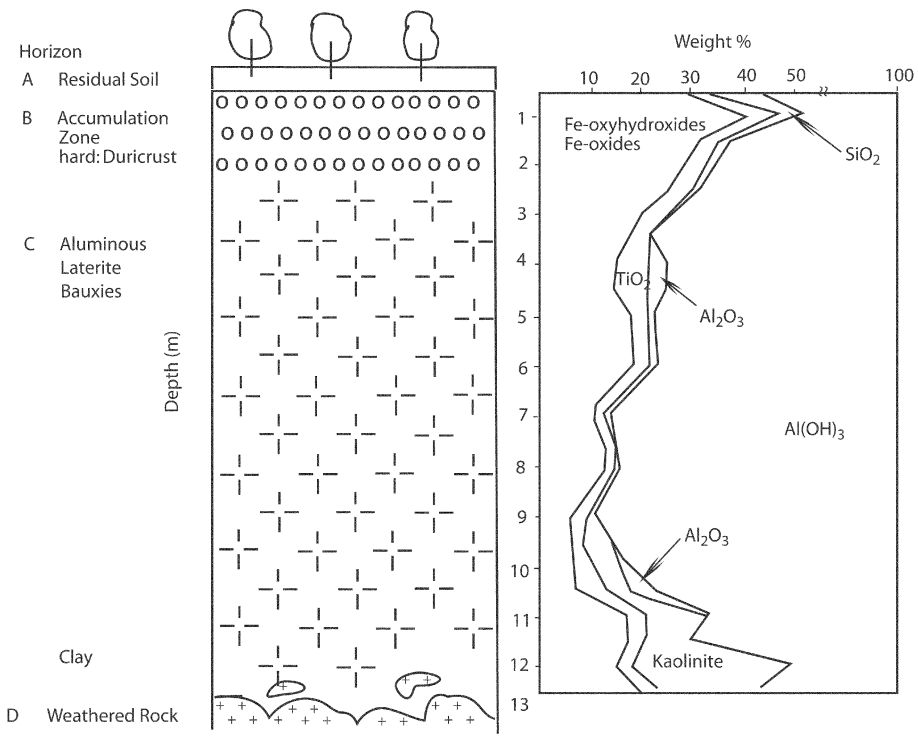

Fig. 7. Vertical section through a laterite deposit in Suriname, South America based on samples collected at 0.5 m intervals. Figure is slightly modified from Topp et al. (1984).

Well over half the dissolved load (in moles) is silica, produced by the continued degradation of the cation-poor clays to kaolinite and gibbsite (Reactions 7 and 17). Note that Reaction 17 does not consume protons (and thus CO_2) since the reactant is free of major soluble cations. Weathering is extremely intense, with complete destruction of all but the most refractory minerals, even though the areal yields or fluxes are extremely low. The net CO_2 consumption or proton fixation rates, ϕCO_2, are equivalent, by charge balance to the total cationic fluxes (Fig. 5).

On high-latitude shields, even in the absence of glaciation, frost weathering processes (Fig. 8) continuously expose fresh rock surfaces and generate gravel, pebble and sand sized material which dominate the bedload in the headwaters. They accelerate both chemical and especially mechanical weathering (Pewe, 1975; Kalvoda, 1992). Sand bars and mounds are found ubiquitously in the middle reaches of the Lena River in Eastern Siberia (Fig. 8d). Little silt-size material is observed either in the river suspended matter or in over-bank flows. Gelifluction destabilizes any protective regolith that may form. It is not surprising that saprolites generated during the warm humid Tertiary (LaSalle et al., 1985) are preserved only in protected areas in the high latitudes.

The 9% volume expansion in situ accompanying phase change from water to ice is only a small part of the explanation for frost weathering. More important is the growth of segregation ice or ice lenses. Water in unfrozen rock migrates to the freezing front due to chemical potential gradients. It accumulates in the microcracks at the freezing front and freezes to ice. The progressive growth of the ice lenses wedge open the microcracks and lead to heaving and shattering (Walder and Hallet, 1985) (Fig. 9). Compared to tropical rivers, Ca and bicarbonate are high and Si is low in the dissolved load. This is consistent with preferential weathering of Ca-plagioclase rather than K-silicates and only the most superficial reaction where labile surficial cations are exchanged for protons with little clay formation.

3.2. Complexity of River Studies

Large uncertainties (not less than 20%) accompany the results presented in Figures 5 and 6 and are inherent in river studies. First, the water discharge can be highly seasonal and varies from year to year, though sensitivity to local weather events is minimized in large river systems. The data in literature are usually from one time sampling at rising or falling stages of the river. The question can be asked if that introduces a bias, e.g. the spring peak discharge from ice-melt is not sampled in the case of arctic basins, and relative contribution from tributaries draining different lithologies may change with season. The sampling strategy has usually been to compensate for the temporal resolution with detailed spatial sampling.

The lithology of a given basin is very rarely of one rock type, and reaction rates differ widely. If trace amounts of carbonate or evaporite are present in a nominally "shield" terrain and their contribution to the dissolved load erroneously included in calculations of aluminosilicate weathering, the rate of CO_2 uptake will be overestimated. Efforts are expended to minimize this by careful examination of

Fig. 8. The Lena River drainage basin in eastern Siberia. (**a**) An ice wedge in peat exposed along the banks of the lower Lena. This particular one is about 1 m in size, but in parts of Siberia they can attain considerable dimensions—3 to 4 m wide near the surface and extending downwards for 5 to 10 m. Because of the cold temperatures, plant roots have been preserved against decay. (**b**) Small pingos in lower Lena. Melting of the inner core of ice by warmer river water and gelifluction lead to their collapse near the banks. (**c**) Ground ice exposed along the bank of the lower Lena. The trees trunks are slim due to the short growing season, and the soil layer is thin. (**d**) Eolian sand is prominent especially in the middle reaches of the Lena. (**e**) Log houses in an early Russian settlement. They are complete with three layered windows and thick padded doors. Because of the instability of the active layer associated with the melt-freeze cycles, log houses are built with felt in between the logs to function as lubricant. This results in crooked appearance but ensures survival of the structure from year to year. During the short summer growing season potatoes and vegetables are grown in raised platform gardens. Pylons and modern buildings are built on concrete platforms to protect against movement of the active layer. (**f**) Notice the very sharp tree line along the bank cut by the bulldozer action of the spring ice melt. In southern Siberia taiga forest is dense but tree trunks tend to be very thin due to short summers.

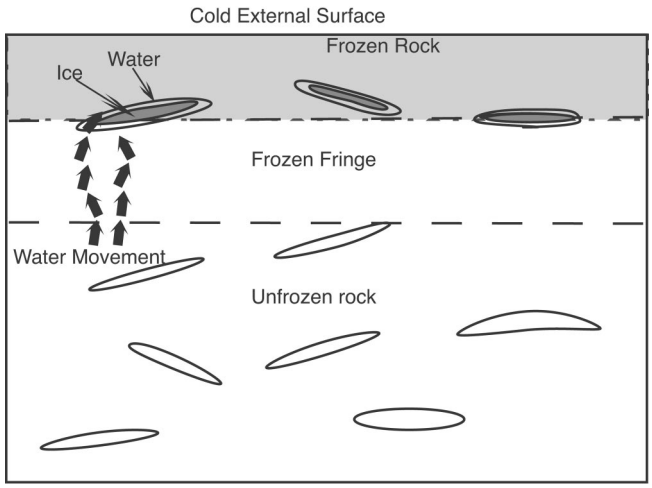

Fig. 9. A cartoon showing freezing of cracked rock. Water in unfrozen rock migrates through the frozen fringe to growing ice-filled cracks. Figure modified from Walder and Hallet (1985).

fluvial chemical composition.

The weathering rates calculated represent the *integrated* weathering signal from the bedrock, soil, vegetation, atmospheric deposition of local origin, and floodplain storage if any. Essentially, the comparison here is between the weathering of bedrock at high latitudes with its integral taiga or tundra vegetation and frozen soils and that of bedrock in the low latitudes with its rain forest and lateritic regolith. The effect of soil and vegetation cannot be isolated using the major elements and Sr isotope data set alone.

Flow rates in the main channels of swift rivers are on the order of a few km/h. In the case of a large river with a length of ~4000 km, it takes about a month for a parcel of water to travel from the headwaters to the mouth. Therefore, the flux calculations presented above are a snapshot of the delivery at present. A subtler question is whether the susceptibility to weathering is purely a result of present climate or is a remnant effect of past environment. This question has significance especially for high latitude rivers that have experienced warm humid climates at lower paleo-latitudes. In the tropical shields, weathering is presently at steady state, and a mass balance is attained between the bedrock and the solid and dissolved weathering products. The "fluvial isochron" of the Rb-Sr system is one evidence. In formerly glaciated basins like the Mackenzie River, measurement of uranium decay series ($^{234}U/^{238}U$, $^{230}Th/^{238}U$, $^{226}Ra/^{238}U$) in the dissolved and suspended loads show that the current fluvial fluxes are still under the impact of the last glaciation (Vigier et al., 2001).

3.3. Comparison to Watershed–Scale Studies

This paper focuses on large rivers (drainage area >> 100 km^2), because they integrate over regional areas and are thus more applicable to discussions on the global carbon cycle. However, watershed-scale (0.1 to 10 km^2) studies are informative, as the lithologic control is thought to be tighter. White and Blum (1995) amassed data for 62 watersheds underlain by granitoid rocks and found an Arrhenius type temperature dependence with apparent activation energy of 59 kJ/mol (Equation 3). The authors note that the watersheds treated are geographically limited to mostly Europe and North America, and the data were originally obtained to characterize acid deposition, deforestation, nutrient cycling, etc. Perturbation by acid rain is a strong possibility: 11 out of the 62 watersheds had very acidic pH (4.52 to 4.90) and 19 didn't have pH values reported.

Studies of the chemical transport of small glacier-fed streams in igneous and metamorphic rocks (Sharp et al., 1995; Anderson et al., 1997) show that even under ice, the weathering rates are substantial in temperate glaciers. Like the high latitude shield rivers, these glacial streams are Ca-HCO_3 dominated and suggest superficial weathering of easily weathered lithologies.

3.4. Importance of Basalt Weathering

Conclusions supporting weak to non-existent climate dependence of silicate weathering have also been reached by Bluth and Kump (1994) in a comparative study of mainly transport limited volcanic terrains in Hawaii, western U.S. and Iceland, where runoff, vegetation cover and temperature vary widely. However, Dessert et al., (2002) based on the data set shown in Figure 6 find a good fit to the Arrhenius equation (Equation 3) but with lower E_a (42 kJ/mol) than the 68 kJ/mol assumed in Berner and Kothavala (2001). While basalt weathering indeed contributes disproportionately to chemical weathering rate or CO_2 drawdown because of its lability, they are areally more restricted than basement exposures. For it to single-handedly drive the negative feedback, continued exposure of basalt of significant areal extent through geologic time is required. Today the flood basalt provinces, hot spots or island arcs are the main loci of basalt weathering. As these features are generated by plate tectonics unrelated to surface environmental conditions, it is difficult to expect the temperature dependence of basalt weathering to explain the stability of climate over geologic timescales.

3.5. Implications for the Phanerozoic Evolution of Atmospheric CO_2

In the present situation of the Guayana and Aldan shields the physical exposure mechanism is primarily responsible for the rate of continental weathering. When fresh bedrock of low relief is initially exposed via uplift, weathering is dependent on climate, especially rainfall. During the late Paleozoic when both Guayana and Aldan shields were experiencing

warm climate, and before the buildup of significant laterite, weathering would initially have been faster where rainfall and temperatures were higher. As the plates moved towards present latitudes, on the hot and humid tropical shields a laterite mantle would quickly have developed (accumulation rate ~5 m/m.y.; Brown et al., 1994). At these rates and without active erosion, a few million years, a short interval on geologic time scales, is enough for the laterite mantle to seal the weathering front. On cooler and drier shield terrains it would take progressively longer for the same amount of cover to form. Then at the latitude and climate condition where frost weathering becomes important, the trend reverses. A new mechanism in the form of frost weathering is available to remove the lateritic regolith and generate fresh surface area, leading to high weathering rates. Thus, the unlikely situation is attained, where tropical shields and arctic shields weather at similar rates.

4. CONCLUSION

It should not be construed that the above results cast doubt on the Arrhenius and Clausius-Clapeyron relationships fundamentally. Rather, what can be emphasized uniquely with global studies that may not be obvious from laboratory experiments or watershed scale surveys is the importance of physical mechanisms of exposure under threshold conditions. Until frost weathering mechanisms become effective, weathering rates are expected to be slower where temperatures and precipitation are low and there is no other relief generating mechanism (e.g., mountain uplift). At low latitudes, until sufficient regolith accumulates, weathering rates will increase with rising temperature and precipitation.

Taken overall, observational fluvial data to date indicate that there is no simple Arrhenius type temperature-dependence or general environmental control on weathering rates. Transport mechanisms (e.g., mountain building, frost shattering) dominate, and there is no continuous relationship between these and climate. A comparison between shield rivers and orogenic zones indicates much higher fluxes for the latter (Huh and Edmond, 1999). This partly supports the idea that increases in global degassing are matched by increases in CO_2 uptake via enhanced weathering accompanying mountain uplift, as in the Himalayas or the Western Cordillera of the Americas (Raymo and Ruddiman, 1992). Orderly heat loss through seafloor spreading and resulting plate tectonics, unique to the Earth, would have to provide a CO_2 source from burial metamorphism and a parallel sink through the exposure of diverse lithologies. The actual mechanism that maintains the balance between slowly varying degassing and seemingly intermittent mountain uplift is an unresolved question.

Some of the current and future directions for research on continental weathering, an important component of the global carbon cycle, are briefly summarized.

In this paper the main focus was on the inorganic portion of the global carbon cycle. However, very little is known about the nature, magnitude, and temporal variation of CO_2 release during weathering of organic-rich reduced sediments. Redox-sensitive, oxyanion forming elements (rhenium, uranium, molybdenum, vanadium, etc.) and isotopic systems related to them ($^{187}Os/^{188}Os$, $^{234}U/^{238}U$) can be informative.

Plants have long been recognized to have an effect on weathering. However, quantitative measurement of that effect has remained elusive. Release of organic acids increases weathering rates, but recycling by the above-ground biomass and decreasing permeability of the soil decrease the chemical loading of rivers. Remote sensing of different vegetation groups at drainage basin scales, combined with fluvial flux data may complement the mass balance approaches using sand boxes and laboratory batch experiments.

The application of uranium decay series provides new insight to erosion timescales, whereas weathering has previously been assumed to be at steady state.

Developing weathering proxies is important in order to reconstruct a record of past continental weathering and Phanerozoic CO_2 levels. For example, the highs in the marine $^{87}Sr/^{86}Sr$ record are interpreted as periods of continental input of extremely radiogenic Sr at high flux during Himalayan type orogenies (continent-continent collision) and the lows as input of predominantly mantle Sr through oceanic hot springs. Likewise, marine Os isotope record is an interplay between continental weathering of organic-rich reduced sediments and hydrothermal input at mid-ocean ridges.

ACKNOWLEDGMENTS: The Hydrology and Chemical Oceanography programs of the U.S. National Science Foundation provided past and ongoing financial support. The author thanks John M. Edmond for stimulating discussions.

REFERENCES

Åberg, G. and Wickman, F.E., 1987, Variations of $^{87}Sr/^{86}Sr$ in water from streams discharging into the Bothnian Bay, Baltic Sea. Nordic Hydrology, 18, 33–42.

Ambrosi, J.P. and Nahon, D., 1986, Petrological and geochemical differentiation of lateritic iron profile. Chemical Geology, 57, 371–393.

Anderson, S.P., Drever, J.I. and Humphrey, N.F., 1997, Chemical weathering in glacial environments. Geology, 25, 399–402.

Andersson, P.S., Wasserburg, G.J., Ingri, J. and Stordal, M.C., 1994, Strontium, dissolved and particulate loads in fresh and brackish waters: the Baltic Sea and Mississippi Delta. Earth and Planetary Science Letters, 124, 195–210.

Berner, R.A., 1978, Equilibrium, kinetics and the precipitation of magnesian calcite from seawater. American Journal of Science, 278, 1435–1455.

Berner, R.A. and Kothavala, Z., 2001, GEOCARB III: A revised model of atmospheric CO_2 over Phanerozoic time. American Journal of Science, 301, 182–204.

Berner, R.A., Lasaga, A.C. and Garrels, R.M., 1983, The carbonate-silicate geochemical cycle and its effect on atmospheric carbon

dioxide over the past 100 million years. American Journal of Science, 283, 641–683.

Blum, J.D. and Erel, Y., 1995, A silicate weathering mechanism linking increases in marine $^{87}Sr/^{86}Sr$ with global glaciation. Nature, 373, 415–418.

Bluth, G.J.S. and Kump, L.R., 1994, Lithologic and climatologic controls of river chemistry. Geochimica et Cosmochimica Acta, 58, 2341–2359.

Bourman, R.P., 1993, Models of ferricrete genesis: evidence from southeastern Australia. Zeitschrift Geomorphologie, 37, 77–101.

Brown, E.T., Bourlès, D.L., Colin, F., Sanfo, Z., Raisbeck, G.M. and Yiou, F., 1994, The development of iron crust lateritic systems in Burkina Faso, West Africa examined with in-situ produced cosmogenic nuclides. Earth and Planetary Science Letters, 124, 19–33.

Dessert, C., Dupré, B., François, L.M., Schott, J., Gaillardet, J., Chakrapani, G. and Bajpai, S., 2001, Erosion of Deccan Traps determined by river geochemistry: impact on the global climate and the $^{87}Sr/^{86}Sr$ ratio of seawater. Earth and Planetary Science Letters, 188, 459–474.

Edmond, J.M. and Huh, Y., 1997, Chemical weathering yields from basement and orogenic terrains in hot and cold climates. In: Ruddiman, W.F. (ed.), Tectonic Uplift and Climate Change. Plenum Press, New York, p. 329–351.

Edmond, J.M., Palmer, M.R., Measures, C.I., Grant, B. and Stallard, R.F., 1995, The fluvial geochemistry and denudation rate of the Guayana Shield in Venezuela, Colombia and Brazil. Geochimica et Cosmochimica Acta, 59, 3301–3325.

Huh, Y. and Edmond, J.M., 1999, The fluvial geochemistry of the rivers of Eastern Siberia: III. Tributaries of the Lena and Anabar draining the basement terrain of the Siberian Craton and the Trans-Baikal Highlands. Geochimica et Cosmochimica Acta, 63, 967–987.

Huh, Y., Panteleyev, G., Babich, D., Zaitsev, A. and Edmond, J.M., 1998a, The fluvial geochemistry of the rivers of Eastern Siberia: II. Tributaries of the Lena, Omoloy, Yana, Indigirka, Kolyma, and Anadyr draining the collisional/accretionary zone of the Verkhoyansk and Cherskiy ranges. Geochimica et Cosmochimica Acta, 62, 2053–2075.

Huh, Y., Tsoi, M.-Y., Zaitsev, A. and Edmond, J.M., 1998b, The fluvial geochemistry of the rivers of Eastern Siberia: I. Tributaries of the Lena River draining the sedimentary platform of the Siberian Craton. Geochimica et Cosmochimica Acta, 62, 1657–1676.

Kalvoda, J., 1992, Geomorphological Record of the Quaternary Orogeny in the Himalaya and the Karakoram. Elsevier, Amsterdam, 315 p.

LaSalle, P., De Kimpe, C.R. and Laverdiere, M.R., 1985, Sub-till saprolites in southeastern Quebec and adjacent New England: Erosional, stratigraphic, and climatic significance. Geological Society of America Special Paper, 197, 13–20.

Louvat, P., 1997, Etude géochimique de l'érosion fluviale d'îles volcaniques à l'aide des éléments majeurs et traces. Ph.D. thesis, Université Paris 7, Paris, 322 p. (in French)

Louvat, P. and Allègre, C.J., 1998, Riverine erosion rates on Sao Miguel volcanic island, Azores archipelago. Chemical Geology, 148, 177–200.

Louvat, P. and Allègre, C.J., 1997, Present denudation rates on the island of Réunion determined by river geochemistry: Basalt weathering and mass budget between chemical and mechanical erosions. Geochimica et Cosmochimica Acta, 61, 3645–3669.

Mackenzie, F.T., 2003, Our Changing Planet. Prentice Hall, Upper Saddle River, New Jersey, 580 p.

Martin, C., 1987, Les mesures de l'érosion chimique et interprétation des résultats dans les petits bassins versants de roches cristallines: exemples pris dans le massif des Maures (Var, France). In: Processus et mesure de l'érosion. CNRS, p. 329–348. (in French)

McDowell, W.H. and Asbury, C.E., 1994, Export of carbon, nitrogen, and major ions from three tropical montane watersheds. Limnology and Oceanography, 39, 111–125.

Meybeck, M., 1986, Composition chimique des ruisseaux non pollués de France. Sciences Géologique (Bulletin), 39, 3–77 (in French).

Millot, R., Gaillardet, J., Dupré, B. and Allègre, C.J., 2002, The global control of silicate weathering rates and the coupling with physical erosion: new insights from rivers of the Canadian Shield. Earth and Planetary Science Letters, 196, 83–98.

Négrel, P., Allègre, C.J., Dupré, B. and Lewin, E., 1993, Erosion sources determined by inversion of major and trace element ratios and strontium isotopic ratios in river water: The Congo Basin case. Earth and Planetary Science Letters, 120, 59–76.

Ollier, C.D., 1991, Aspects of silcrete formation in Australia. Zeischrift Geomorphologie, 35, 151–163.

Palmer, M.R. and Edmond, J.M., 1989, The strontium isotope budget of the modern ocean. Earth and Planetary Science Letters, 92, 11–26.

Palmer, M.R. and Edmond, J.M., 1992, Controls over the strontium isotope composition of river water. Geochimica et Cosmochimica Acta, 56, 2099–2111.

Pewe, T.L., 1975, Quaternary Geology of Alaska. U. S. Geological Survey Professional Paper, 835, 145 p.

Raymo, M.E. and Ruddiman, W.F., 1992, Tectonic forcing of late Cenozoic climate. Nature, 359, 117–122.

Sharp, M., Tranter, M., Brown, G.H. and Skidmore, M., 1995, Rates of chemical denudation and CO_2 drawdown in a glacier-covered alpine catchment. Geology, 23, 61–64.

Stallard, R.F. and Edmond, J.M., 1983, Geochemistry of the Amazon 2. The influence of geology and weathering environment on the dissolved load. Journal of Geophysical Research, 88, 9671–9688.

Thomas, M.F., 1994, Ages and geomorphic relationships of saprolite mantles. In: Robinson, D.A. and Williams, R.B.G. (eds.), Rock Weathering and Landform Evolution. John Wiley & Sons Ltd., New York, p. 287–301.

Topp, S.E., Salbu, B., Roaldset, E. and Jorgensen, P., 1984, Vertical distribution of trace elements in lateritic soil. Chemical Geology, 47, 159–174.

Twidale, C.R., 1990, The origin and implications of some erosional landforms. Journal of Geology, 98, 343–364.

Vegas-Vilarrubia, T., Maass, M., Rull, V., Elias, V., Ramon, A., Ovalle, C., Lopez, D., Schneider, G., Depetris, P.J. and Douglas, I., 1994, Small catchment studies in the tropical zone. In: Moldan, B. and Cerny, J. (eds.), Biogeochemistry of Small Catchment: A Tool for Environmental Research. Wiley, U.K., p. 343–360.

Viers, J., Dupré, B., Braun, J.-J., Deberdt, S., Angeletti, B., Ngoupayou, J.N. and Michard, A., 2000, Major and trace element abundances, and strontium isotopes in the Nyong basin rivers (Cameroon): constraints on chemical weathering processes and elements transport mechanisms in humid tropical environments. Chemical Geology, 169, 211–241.

Vigier, N., Bourdon, B., Turner, S. and Allègre, C.J., 2001, Erosion timescales derived from U-decay series measurements in rivers. Earth and Planetary Science Letters, 193, 549–563.

Vinogradov, V.I. and Leytes, A.M., 1987, Rb-Sr dating of the stages of granitization of the South Aldan Shield. In: Shukolyukov, Y.A. (ed.), Isotope Dating of Metamorphic and Metasomatic Pro-

cesses. Nauka, Moscow, p. 103–115.
Wadleigh, M.A., Veizer, J. and Brooks, C., 1985, Strontium and its isotopes in Canadian rivers: Fluxes and global implications. Geochimica et Cosmochimica Acta, 49, 1727–1736.
Walder, J. and Hallet, B., 1985, A theoretical model of the fracture of rock during freezing. Geological Society of America Bulletin, 96, 336–346.
Walker, J.C.G., Hays, P.B. and Kasting, J.F., 1981, A negative feedback mechanism for the long-term stabilization of Earth's surface temperature. Journal of Geophysical Research, 86, 9776–9782.
Wallmann, K., 2001, Controls on the Cretaceous and Cenozoic evolution of seawater composition, atmospheric CO_2 and climate. Geochimica et Cosmochimica Acta, 65, 3005–3025.
Webster, P.J., 1994, The role of hydrological processes in ocean-atmosphere interactions. Reviews of Geophysics, 32, 427–476.
Wedepohl, K.H., 1995, The composition of the continental crust. Geochimica et Cosmochimica Acta, 59, 1217–1232.
White, A.F. and Blum, A.E., 1995, Effect of climate on chemical weathering in watersheds. Geochimica et Cosmochimica Acta, 59, 1729–1747.
White, A.F. and Brantley, S.L., 1995, Chemical Weathering Rates of Silicate Minerals. Reviews in Mineralogy, Volume 31, Mineralogical Society of America, Washington, D.C., 583 p.
White, A.F., Bullen, T.D., Vivit, D.V., Schulz, M.S. and Clow, D.W., 1999, The role of disseminated calcite in the chemical weathering of granitoid rocks. Geochimica et Cosmochimica Acta, 63, 1939–1953.
Wickman, F.E. and Åberg, G., 1987, Variations in the $^{87}Sr/^{86}Sr$ ratio in lake waters from Central Sweden. Nordic Hydrology, 18, 21–32.
Yang, C., Telmer, K. and Veizer, J., 1996, Chemical dynamics of the St. Lawrence riverine system: δD_{H2O}, $\delta^{18}O_{H2O}$, $\delta^{13}C_{DIC}$, $\delta^{34}S_{Sulfate}$, and dissolved $^{87}Sr/^{86}Sr$. Geochimica et Cosmochimica Acta, 60, 851–866.

Manuscript received August 4, 2003
Manuscript accepted August 30, 2003